Iranian Journal of Chemical Engineering
Vol. 12, No. 3 (Summer 2015), IAChE

Research note

Synthesis of SnO_2 and ZnO Nanoparticles and SnO_2-ZnO Hybrid for the Photocatalytic Oxidation of Methyl Orange

A. Ghaderi[1], S. Abbasi[2*], F. Farahbod[3]

Department of Chemical Engineering, Sirjan Branch, Islamic Azad University, Sirjan, Iran

Esfarayen University of Technology, Esfarayen, North Khorasan, Iran

Department of Chemical Engineering, Firoozabad Branch, Islamic Azad University, Firoozabad, Iran

Abstract

The aim of the current research is concentrated on the synthesis of the different nanoparticles such as SnO_2 and ZnO nanoparticles and SnO_2-ZnO hybrid via sol gel method to investigate their photocatalytic applications for removal of methyl orange pollutant in water. Therefore, $ZnCl_2$ and $SnCl_2.2H_2O$ were used as ZnO and SnO_2 source respectively. The samples were characterized by X-ray diffraction (XRD) spectroscopy, Fourier transform infrared spectroscopy (FTIR) and UV-Vis spectroscopy. XRD results revealed that the crystalline structure of SnO_2 and ZnO nanoparticles were formed. FTIR analysis confirmed the presence of ZnO and SnO_2 nanoparticles. Optical properties of samples measured using UV-Vis spectrophotometer and the achieved results demonstrated that the photocatalytic activity of SnO_2-ZnO hybrid for the degradation of methyl orange is higher than that of SnO_2 nanoparticles and lower than that of ZnO nanoparticles. Weight fraction dependence study also showed that the degradation of methyl orange dye increases with weight fraction. The experimental results revealed that after 35 min UV light irradiation, the photocatalytic degradation of MO using 0.5 g ZnO, hybrid of ZnO-SnO_2 and SnO_2 nanoparticles reached to 99.35%, 92.14% and 87.91%, respectively. In addition, maximum removal efficiency of MO was related to the suspension containing of 0.5 g of ZnO hybrid equal to 99.35%.

Keywords: *SnO_2 Nanoparticles, ZnO Nanoparticles, SnO_2-ZnO Hybrid, Photocatalytic Activities, Methyl Orange*

1. Introduction

Contaminations of ground water systems by organic chemicals pose a serious environmental threat. The severity of this threat is due to their toxicity to animals and humans. The ‘‘Environmental Protection Agency’’ (USA) has listed several volatile organic compounds as contaminants in ground water [1]. In recent years,

*Corresponding author: s.abbasi@esfarayen.ac.ir, abasi_1362@yahoo.com

semiconductor photocatalysis has become more and more attractive and important since it has great potential to contribute to such environmental problems. Photocatalysis using nanoparticles has potential applications in solar energy conversion, water splitting and treatment of environmental pollutants [2]. Metal oxide semiconductor photocatalysis, an ideal "green" technology, has attracted extensive attention due to its wide potential applications in environmental protection procedures, such as water disinfection, hazardous waste remediation and water purification [3,4]. Among various semiconductor photocatalysts, tin oxide (SnO_2) nanomaterials, have been expected to be a powerful photocatalyst for the degradation of organic pollutants in aqueous solution due to their excellent properties, such as transparency, high photosensitivity, low cost and environmental friendliness [5,6]. Among inorganic nanoparticles, ZnO is of special importance for the photocatalytic generation of hydrogen peroxide, which can be utilized for the degradation of organic pollutants, and the sterilization of microbial species [7]

The fast recombination rate of the photoexcited electron–hole pairs is the key factor in the process of semiconductor photocatalysis which inhibit the phitocatalytic activitiy of the semiconductors [8]. Therefore, there has been much interest to improve the photocatalytic activity of these semiconductors [9,10].

The previous studies showed that one of the most effective ways to lower the recombination of electron–hole pairs is coupling two semiconductor nanoparticles with different band gap widths [11-13]. There are many reports describing the photocatalytic degration of water pollutants with varous nanoparticles, such as Au [14], Ag- SnO_2 [3], Ag-TiO_2 [15], TiO_2 [16], ZnO-SnO_2 [9,17,18], TiO_2-SnO_2 [19], TiO_2-ZnO [20].

Wang *et al.* [15] investigated the photocatalytic properties of Fe^{3+} doped Ag@TiO_2 core–shell nanoparticles on the photodegration of methyl orange (MO). Their experimental results revealed that the sample with 1.0 wt% Ag achieved the best photocatalytic activity and it is the only sample which has a quicker degradation rate than the sample without Ag cores. Zhang *et al.* [17] have reported the experimental results on the photocatalytic activity of nanosized ZnO–SnO_2 for the degradation of MO. They observed that the coupled oxides ZnO–SnO_2 mainly consist of nanosized ZnO and SnO_2, and they have better photocatalytic activity for the degradation of MO than ZnO or SnO_2 alone. Wang *et al.* [9] have studied the effects of Ag contents of Ag/ZnO-SnO_2 catalysts on improving the photocatalytic activity for the degradation of MO. They reported that after Ag was loaded on the surface of coupled catalysts prepared at pH 7, the photocatalytic performance of catalysts was greatly improved. The optimum Ag loading amount was found to be around 3%. The activity of 3% Ag/ZnO-SnO_2 catalyst was higher than that of the pure ZnO catalyst and the ZnO-SnO_2 coupled catalyst prepared at pH 7 by 84 and 88%, respectively. Yang *et al.* [5] have reported the photocatalytic activity of SnO_2/ZnO/TiO_2 composite photocatalysts for the degradation of MO. Their experimental results showed that the formation of the rutile phase at the high Sn–

Zn doping level is an important factor to result in a significant decrease of the catalytic decomposition of MO. Also, they observed that the maximum degradation yield of SnO_2/ZnO/TiO_2 approaches to 85% after 40 min irradiation. Chen *et al.* [21] studied the photocatalytic activities of Ag-ZnO and Au–Ag- ZnO for photodegradation of MO under UV irradiation. They reported that during 180 min irradiation, the MO concentration in the absence of photocatalyst reduced about only 15.4%, while the pure ZnO shows activity in photocatalytic MO, and the degradation efficiency of MO is 30.1% in 180 min. Ag-ZnO represents significant photocatalytic characteristic for MO degradation. The efficiency reaches up to 40%. In the Au–Ag-system, the degradation efficiency is 52.5%. The modification of Au and Ag significantly enhanced the photocatalytic activity of ZnO.

Although photocatalitic activity of many nanoparticles has been investigated by many researchers, the effect of concentration of nanoparticles has been reported so far. Therefore in this study, we want to report for the first time the effect of concentration of SnO_2 and ZnO nanoparticles and SnO_2-ZnO hybrid on the removal efficiency of methyl orange.

2. Materials and experimental

For preparation of the synthesized SnO_2 and ZnO nanoparticles and SnO_2-ZnO hybrid the following materials were used:

Zinc Chloride ($ZnCl_2$, M=136.30, Merck), stannous chloride dehydrate ($SnCl_2.2H_2O$, M=225.63, Scharlau), NaOH (Merck) and Ammonia solution (25%, Merck).

SnO_2 nanoparticles used in this study have been prepared by means of dissolving of 2 g $SnCl_2.2H_2O$ in 100 mL distilled water. After complete dissolution, 1 mL ammonia solution was added dropwise to the above solution under vigorous stirring. The resulting gels were filtered and dried at 80ºC for 24 h in order to remove water molecules. Finally, tin oxide nanoparticles were formed by calcination at 550ºC for 2 h.

ZnO nanoparticles was synthesized according to Ramachandran *et al.* method [22]. Typically, 3 g $ZnCl_2$ without any further purification was added to 100 mL distilled water at 90°C under vigorous stirring. Then 16 mL of 5 M NaOH aqueous solution was added dropwise to the zinc chloride solution along with vigorous stirring of the solution while the temperature of the solution was maintained at 90ºC. Finally, ZnO nanoparticles separate from the solution using filtration dried at room temperature and calcined at 300℃ for 3 h.

SnO_2-ZnO hybrid was synthesized by the following procedure:

0.3 g of synthesized SnO_2 nanoparticles dissolved to 34 mL distilled water with continuously sonicated for 10 min at 90℃, then 1g $ZnCl_2$ without any further purification was added to solution while the temperature of the solution was maintained at 90ºC. Then 5.34 mL of 5 M NaOH aqueous solution was added dropwise to the mixed solution. Finally, SnO_2-ZnO hybrid separate from the solution using filtration dried at room temperature and calcined at 300℃ for 3h.

X-ray powder diffraction was performed to characterize the phase composition and crystal structure of the samples, using PHILIPS-binary equipment as well as a

Bruker D8 Advance (40 kV/30 mA) with Cu Kα (1.542 A°) radiation. The scanning velocity was 0.02°/s, and the 2θ range scanned ranged from 2° to 90°. The crystalline sizes of the nanoparticles were determined by the Scherrer formula (Eq. 1), using a K factor of 0.9:

$$B = \frac{K\lambda}{\beta \cos\theta} \quad (1)$$

where B is crystalline size, in nm; λ wavelength for the radiation is used, which is 1.5406 A° for Cu; β: full width at half maximum intensity (FWHM); θ: angle for the XRD maximum peak. FTIR measurements synthesized nanoparticles in the range of 400-4000 cm^{-1} were carried out on a Tensor 70 Fourier transform infrared spectrometer. The photocatalytic activity of each sample was evaluated in terms of the degradation of methyl orange. MO was selected as a model pollutant because it is a common contaminant in industrial wastewater and it has good resistance toward light degradation [15]. The certain amount of photocatalyst (0.25, 0.5 g) was added into a 80-mL quartz photoreactor containing 60 mL of a 10 mg/L MO solution. The mixture was stirred for 60 min in the dark in order to reach the adsorption–desorption equilibrium. A 150-W high-pressure Hg lamp was used as a UV light source. At given time intervals (After every 5 min), the analytical samples were taken from the mixture and immediately centrifuged and then filtered to remove the particles. The concentration of the filtrate was analyzed by checking the absorbance at the maximum band 464 nm of MO to determine the concentration of MO 464 nm with a UV–vis spectrophotometer (Lambda EZ 201, Perkin Elmer company).

UV–vis absorption spectra monitoring the change in concentration of the organic dyes were periodically recorded. The absorbance A_0 measured after stirring for 1 h in the dark was taken as the initial concentration C_0 of the solution. The absorbance A_t measured after variable periods of illumination was taken as corresponding to the residual concentration C_t. The degree of organic compound degradation was calculated by Eq. 2, [21].

$$\text{Removal efficiency } (\%) = \frac{C_0 - C_t}{C_0} \times 100 = \frac{A_0 - A_t}{A_0} \times 100 \quad (2)$$

3. Results and discussion

3.1. X-ray diffraction

Fig. 1 and 2 show the XRD patterns of synthesized ZnO and SnO_2 nanoparticles, respectively.

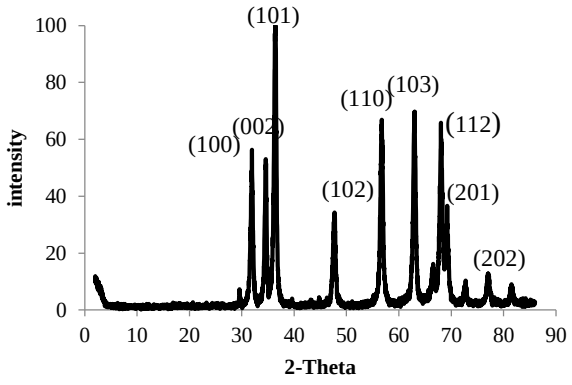

Figure 1. XRD pattern of ZnO nanoparticles.

The XRD pattern of ZnO nanoparticles (Fig. 1) revealed that the characteristic peaks

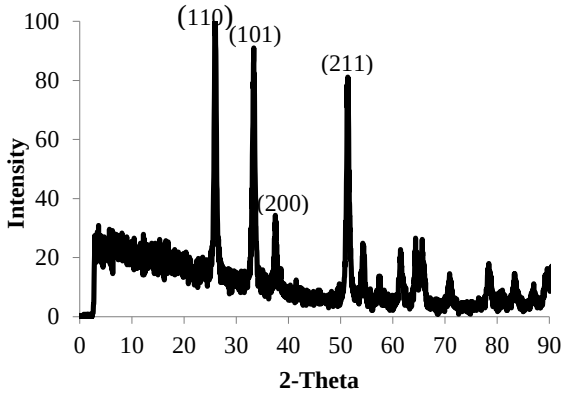

Figure 2. XRD pattern of SnO_2 nanoparticles.

at 31.96°, 34.57°, 36.50°, 47.77°, 56.71°, 62.98°, 68.02°, 69.28° and 77.07° corresponding to the (100), (002), (101), (102), (110), (103), (112), (201) and (202) Bragg reflection planes, respectively. Meanwhile, the XRD results revealed that the ZnO nanoparticles possess hexagonal wurtzite phase with lattice constants *a* and *b*=3.22 A° and *c*=5.2 A°, which are good agreement with other literature [21,22,23]. As XRD analysis confirmed, the average crystallite size of the ZnO nanoparticles is about 10.5 nm in accordance with the results calculated using the Scherrer equation which was mentioned in Eq (1).

The XRD pattern of the SnO_2 nanoparticles (Fig. 2) demonstrated that the peaks at 2θ values of 26.57°, 33.77°, 37.76°, 51.75°, 61.74°, and 65.74° can be associated with (110), (101), (200), (211), (310), and (301), respectively. Meanwhile, the XRD results revealed that the SnO_2 nanoparticles possess tetragonal structure with lattice constants *a* and *b*= 4.75 A° and *c*=3.19 A°, and with the average crystallite size of 9.64 nm.

Fig. 3 shows the XRD patterns of synthesized SnO_2-ZnO powder. As can be seen, the crystalline of ZnO have been successfully formed on the outer surface of SnO_2 nanoparticles. Meanwhile, the XRD results revealed that, the characteristic peaks of SnO_2 and ZnO nanoparticles became intensified and sharpened, indicating that the crystalline of SnO_2-ZnO powder became much more perfect.

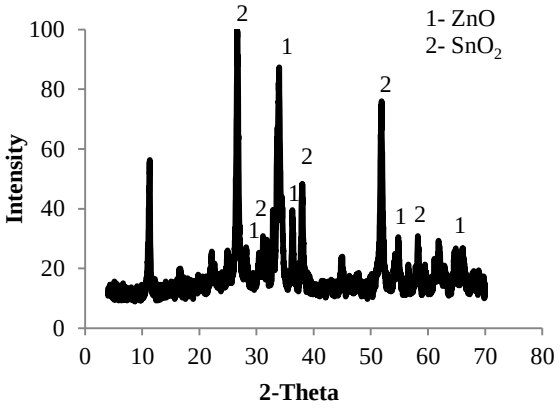

Figure 3. XRD pattern of SnO_2-ZnO hybrid.

3-2. FT-IR analysis

Fourier transform infrared (FTIR) analysis was performed to confirm the presence of functional groups on the surface of samples. Fig. 4 demonstrates FTIR spectra of SnO_2 nanoparticles. Absorbance band around at 623 cm^{-1} could be attributed to O-Sn-O, Sn-O or O-Sn-O lattice, which is consistent with the results obtained by Chetri *et al.* [24]. Also, the infrared spectra indicates that the absorptions at 3446 cm^{-1} are evidently related to the presence of hydroxyl groups of water molecules [25] on the outer surface of SnO_2 nanoparticles.

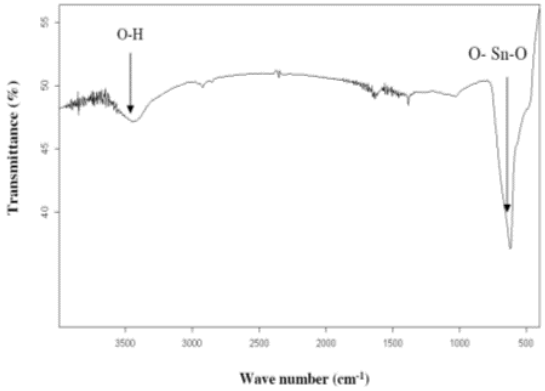

Figure 4. FTIR spectra of SnO_2 nanoparticles.

Fig. 5 shows the FTIR spectra of ZnO nanoparticles. As can be seen, the appearance of peak at 480 cm^{-1} clearly indicates the formation of ZnO nanoparticles which is corroborated by Hariharan [1]. In addition, an absorbance band at 3442 cm^{-1} appears in the IR spectrum of ZnO nanoparticles which attribute to the O-H confirming the presence of hydroxyl groups on the outer surface of ZnO nanoparticles.

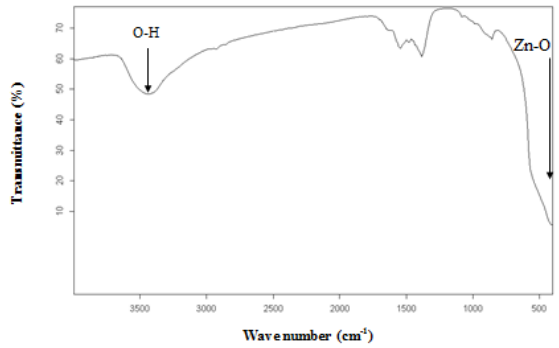

Figure 5. FTIR spectra of ZnO nanoparticles.

Fig. 6 indicates the FTIR spectra of SnO_2-ZnO powder. It is clear that an absorbance band at 480 cm^{-1} and 623 cm^{-1} appears in the IR spectrum of SnO_2-ZnO powder which contributes to the ZnO and O-Sn-O confirming the presence of ZnO and SnO_2 nanoparticles.

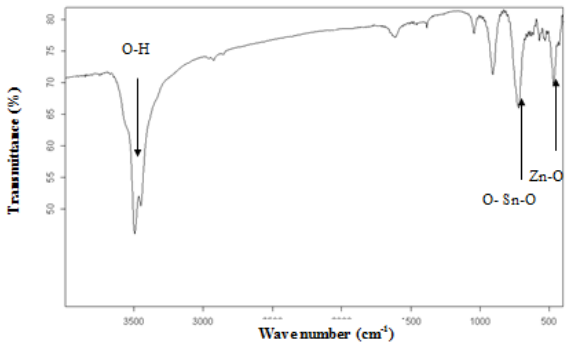

Figure 6. FTIR spectra of SnO_2-ZnO hybrid.

3-3. Photocatalytic activity

Fig. 7 demonstrates the photocatalytic degradation of MO in SnO_2 suspension under UV light irradiation. As can be seen, the removal efficiency of MO increased with increasing the time of irradiation and the weight of SnO_2 nanoparticles. The comparison of the photocatalytic degradation of MO corroborated that the removal efficiency of MO with 0.5 g SnO_2 nanoparticles (94.67%) is higher than that of 0.25 g SnO_2 nanoparticles (84.5%) at the end of irradiation process (50 min). It can be due to the amount of electron-hole pairs which formed during the UV light irradiation. Therefore, by increasing the weight fraction of SnO_2 nanoparticles from 0.25 to 0.5 g, the produced electron-hole pairs and photocatalytic degradation of MO was increased.

Fig. 8 depicts the Photocatalytic degradation of MO in ZnO suspension as a function of irradiation time at two different mass fractions of ZnO nanoparticles. The results show that the removal efficiency of MO increased with respect to the time of irradiation and the weight of ZnO nanoparticles. In the weight of ZnO nanoparticles ranging from 0.25 to 0.5 g and

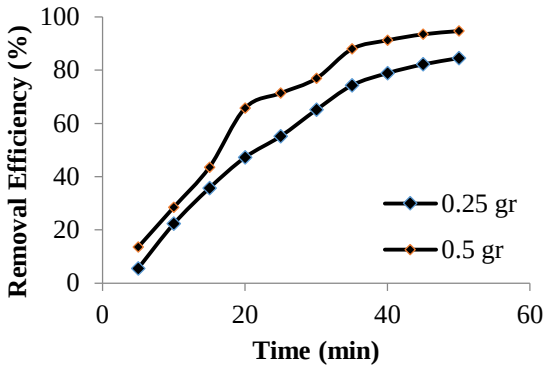

Figure 7. Photocatalytic degradation of MO in SnO_2 suspension, influence of concentration.

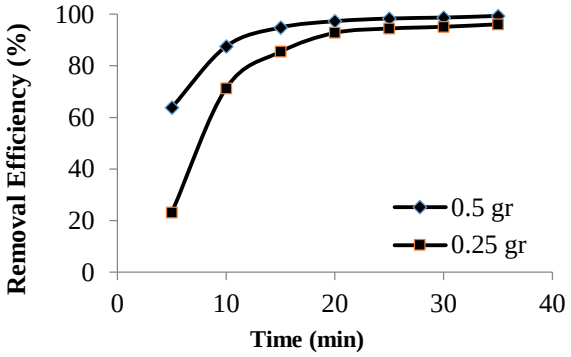

Figure 8. Photocatalytic degradation of MO in ZnO suspension, influence of ZnO nanoparticles content.

UV light irradiation observed that the removal efficiency varied between 23.17% and 99.35%. From Fig. 4 it can be inferred that the maximum removal efficiency of MO in ZnO suspension containing 0.25 g and 0.5 g of ZnO nanoparticles is equal to 96.1% and 99.35%, respectively. Therefore, it can be deducted that the Photocatalytic degradation of MO increases as ZnO nanoparticles content increases.

The photocatalytic activity of SnO_2-ZnO hybrid suspension containing various amount of hybrid is presented in Fig. 9. It is clear that in both suspensions (containing 0.25 g and 0.5 g of SnO_2-ZnO hybrid) photocatalytic degradation of MO increased with respect to the irradiation time. From Fig. 9 it can be inferred that the least removal efficiency of MO for suspension containing SnO_2-ZnO hybrid was recorded for suspension containing 0.25 g of SnO_2-ZnO hybrid equal to 15%. In addition, maximum removal efficiency of MO was related to the suspension containing 0.5 g SnO_2-ZnO hybrid equal to 92.14%. Whereas Yang *et al.* [5] have reported that the maximum degradation yield of SnO_2/ZnO/TiO_2 for the degradation of MO approaches to 85% after 40 min irradiation. This difference may be due to the concentration of nanocomposite.

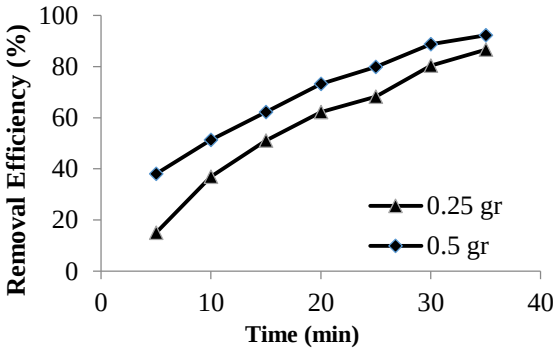

Figure 9. Photocatalytic degradation of MO in SnO_2-ZnO hybrid suspension, influence of SnO_2-ZnO hybrid content.

The comparison between photocatalytic activity of SnO_2 nanoparticles, ZnO nanoparticles and SnO_2-ZnO hybrid illustrated in Fig. 10. As can be deducted from this figure, photocatalytic activity of ZnO nanoparticles is higher than that of SnO_2 nanoparticles. It can be related to the band gap of each nanoparticles. SnO_2 nanoparticles have a wide band gap (3.8 eV) [3,5]. Therefore, SnO_2 nanoparticles need a large amount of UV radiation to excite electron–hole pairs. But ZnO nanoparticles have band gap around 3.25 ev [26]. The

little band gap of ZnO nanoparticles lead to the faster excitation of electron-hole pair. Therefore, the oxidation of organic pollutant and photocatalytic activity increased. As can be seen, after 35 min UV light irradiation, the photocatalytic degradation of MO using 0.5 g ZnO and SnO_2 nanoparticles reached to 99.35% and 87.91%, respectively. Meanwhile, the comparison between photocatalytic activity of single nanoparticles (ZnO and SnO_2 nanoparticles) and hybrid nanoparticles (SnO_2-ZnO nanoparticles) showed that the sequence of photocatalytic degradation of MO containing 0.5 g of each nanoparticle is as ZnO > SnO_2-ZnO > SnO_2. It can be inferred that the photocatalytic activity of SnO_2-ZnO hybrid is higher than that of SnO_2 nanoparticles and lower than that of ZnO nanoparticles. A factor contributing to the enhanced photocatalytic activity of SnO_2-ZnO hybrid rather than SnO_2 nanoparticles is presentation of ZnO with lower band gap in the hybrid. Therefore, at the same time of UV radiation the amount of produced electron–hole pairs in the case of SnO_2-ZnO hybrid is higher than that of SnO_2 nanoparticles. This led to increasing the oxidation of MO and photocatalytic activity of SnO_2-ZnO hybrid.

The results also showed that the photocatalytic activity of SnO_2-ZnO hybrid is lower than that of ZnO nanoparticles. This can be duo to the SnO_2 nanoparticles being decorated by ZnO nanoparticles. Therefore, SnO_2 nanoparticles could not prevent the fast recombination of photo-generated electron/hole pairs. This led to the release of energy in the form of unproductive heat or photons [27], which is not consistent with the results obtained by Wang *et al.* [9]. Because they synthesized the hybrid of ZnO- SnO_2, whereby ZnO act as core and SnO_2 nanoparticles act as shell.

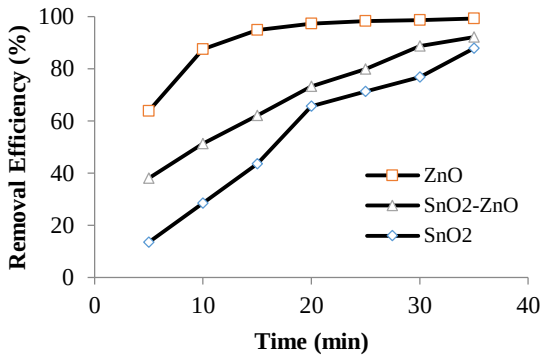

Figure 10. Comparison the photocatalytic activity of SnO_2 nanoparticles, ZnO nanoparticles and SnO_2-ZnO hybrid at 0.5 g of nanoparticles.

4. Conclusions

In the current research we synthesized the SnO_2 and ZnO nanoparticles and SnO_2-ZnO hybrid and investigated the photocatalytic activity of them for degration of methyl orange polluntant in water. The XRD results that the ZnO nanoparticles possess hexagonal wurtzite phase with the average crystallite size of 1.05 nm and the SnO_2 nanoparticles shows tetragonal structure, with the average crystallite size of 0.64 nm. The XRD patterns of synthesized SnO_2-ZnO powder showed that the crystalline of ZnO have been successfully formed on the outer surface of SnO_2 nanoparticles. The results confirmed that the removal efficiency of MO increased with increasing the time of irradiation and the weight of ZnO and SnO_2 nanoparticles and SnO_2-ZnO hybrid. Meanwhile, photocatalytic activity of ZnO nanoparticles is higher than that of SnO_2 nanoparticles and SnO_2-ZnO hybrid.

References

[1] Hariharan, C., "Photocatalytic degradation of organic contaminants in water by ZnO nanoparticles: Revisited", *Appl. Catal., A: General* **304**, 55 (2006).

[2] Zhou, N. Polavarapu, L. Gao, N. Pan, Y. Yuan, P. Wang, Q. and Xu, Q. H., "TiO_2 coated Au/Ag nanorods with enhanced photocatalytic activity under visible light irradiation", *Nanoscale*, (2013).

[3] Liu, H. Liu T. Dong, X. Hua, R. and Zhu, Z. "Preparation and enhanced photocatalytic activity of Ag-nanowires@SnO_2 core–shell heterogeneous structures", *Ceram. Int*. **40**, 16671 (2014).

[4] Wang, X. Fan, H. Q. and Ren, P. R. "Elf-assemble flower-like SnO_2/Ag hetero-structures: correlationamongcomposition,structureandphotocatalytic activity", *S, Colloids Surf., A*, **419**, 140 (2013).

[5] Yang, G. D. Yan, Z. F. and Xiao, T. C., "Preparation and characterization of SnO_2/ZnO_2/TiO_2 composite semiconductor with enhanced photocatalytic activity", *Appl. Surf. Sci* **258**, 8704 (2012).

[6] Yin, K. Shao, M. W. Zhang, Z. S. and Lin, Z. Q., "A single-source precursor route to Ag/SnO_2 heterogeneous nanomaterials and its photocatalysis in degradation of Conco Red, Mater", *Res. Bull*, **47**, 3704 (2012).

[7] Saravanan, R. Kumar, G. V. Narayanan, V. and Stephen, A., "Comparative study on photocatalytic activity of ZnO prepared by different methods", *J. of Mol. Liq., 181, **133*** (2013).

[8] Linsebigler, A. L. Lu, G. and Yates, J. T., "Photocatalysis on TiO_2 surfaces: principles, mechanisms, and selected results", *Chem. Rev.* **95**, 735 (1995).

[9] Wang, H. Baek, S. Lee, J. and Lim, S., "High photocatalytic activity of silver-loaded ZnO-SnO_2 coupled catalysts", *Chem. Eng. J*. **146**, 355 (2009).

[10] Robert, D., "Photosensitization of TiO_2 by MxOy and MxSy nanoparticles for heterogeneous photocatalysis applications", *Catal. Today*, **122**, 20 (2007).

[11] Akurati, K. K. Vital, A. Dellemann, J. Michalow, K. Graule, T. Ferri, D. and Baiker, A. "Flame-madeWO_3/TiO_2 nanoparticles: relation between surface acidity, structure and photocatalytic activity", *Appl. Catal. B: Environ*., **79**, 53 (2008).

[12] Wang, W. W. Zhu, Y. J. and Yang, L. X., "ZnO-SnO_2 hollow spheres and hierarchical nanosheets: hydrothermal preparation, formation mechanism, and photocatalytic properties", *Adv. Funct. Mater*., **17**, 59 (2007).

[13] Li, H. H. D. Ohashi, N. Hishita, S. and Yoshikawa, Y., "Synthesis of nanosized nitrogen-containing MOx–ZnO (M=W, V, Fe) composite powders by spray pyrolysis and their visible-light-driven photocatalysis in gas-phase acetaldehyde decomposition", *Catal. Today*, **93**, 895 (2004).

[14] Ayati, A. Ahmadpour, A. Bamoharram, F. F. Heravi, M. M. and Rashidi, H., "Photocatalytic synthesis of gold nanoparticles using preyssler acid and their photocatalytic activity", *Chin. J. Catal*., **32**, 978 (2011).

[15] Wang, W. Zhang, J. Chen, F. He,

D. and Anpo, M., "Preparation and photocatalytic properties of Fe3+-doped Ag@TiO_2 core–shell nanoparticles", *J. Coll. Inter. Sci*., **323**, 182 (2008).

[16] Ahmed, A. A. E. Hassan, M. A. S. and Kamal, A. M., "Preparation and using of TiO_2 nanoparticles for treatment of water containing formic acid or coliform bacteria", *Nanosci. Nanotechnol.*, **3**, 90 (2013).

[17] Zhang, M. Sheng, G. Fu, J. An, T. Wang, X. and Hu, X., "Novel preparation of nanosized ZnO-SnO_2 with high photocatalytic activity by homogeneous co-precipitation method", *Mater. Lett*. **59**, 3641 (2005).

[18] Wen, Z. Wang, G. Lu, W. Wang, Q. Zhang, Q. and Li, J., "Enhanced photocatalytic properties of mesoporous SnO_2 induced by low concentration ZnO doping", *Cryst. Growth Des*., **7, 1722**(2007).

[19] Shi, L. Li, C. Gu, H. and Fang, D., "Morphology and properties of ultrafine SnO2-TiO2 coupled semiconductor particles", *Mater. Chem. Phys*., **62**, 62 (2000).

[20] Liao, S. Huang, D. Yu, D. Su, Y. and Yuan, G., "Preparation and characterization of ZnO/TiO_2, SO_4^{-2}/ZnO/TiO_2 photocatalyst and their photocatalysis", *J. Photochem. Photobiol. A: Chem*., **168**, 7 (2004).

[21] Chen, L. Huang, T. T. T, C. A. Li, J. Yuan, L. and Cai, Q., "Synthesis and photocatalytic application of Au/Ag nanoparticle-sensitized ZnO films", *Appl. Surf. Sci*., **273**, 82 (2013).

[22] Ramachandran, D. Brijitta, J. Raj, N. N. Jayanthi, V. and Rabel, A. M., "Synthesis and Characterization of Zinc Oxide Nanorods", Int. Conf. on Advanced Nanomaterials & Emerging Engineering Technologies, New Delhi, India, 2013.

[23] Zhang, Y. C. Wu, X. Hu, X. Y. and Guo, R., "Low-temperature synthesis of nanocrystalline ZnO by thermal decomposition of a ‘‘green’’ single-source inorganic precursor in air", *J. Cryst. Growth*, **280**, 250 (2005).

[24] Chetri, P. and Choudhury, A., "Investigation of optical properties of SnO_2 nanoparticles", *Physica E*, **47** 257(2013).

[25] Abbasi, S. Zebarjad, S. M. Baghban, S. H. N. and Youssefi, A., "Synthesis of TiO2 nanoparticles and decorated Multi-walled carbon nanotubes with various content of rutile titania", Synthesis and Reactivity in Inorganic, Metal-Organic, and Nano-Metal Chemistry (2015).

[26] Balachandran, S. Selvam, K. Babub, B. and Swaminathan, M., "The simple hydrothermal synthesis of Ag–ZnO–SnO_2 nanochain and its multiple applications†", *Dalton Trans*., **42**, 16365 (2013).

[27] Xie, Y. Heo, S. H. Yoo, S. H. Ali, G. and Cho, S. O., "Synthesis and Photocatalytic Activity of Anatase TiO_2 Nanoparticles-coated Carbon Nanotubes", *Nanoscale Res.*, **5**, 603 (2010).